6586 *J. Phys. Chem. A* **2008,** *112,* 6586–6591

Decomposition of Hydrofluorocarbons in a Dielectric-Packed Plasma Reactor

Y. S. Mok,*,[†] V. Demidyuk,[‡] and J. C. Whitehead[‡]

Department of Chemical Engineering, Cheju National University, Aradong, Jeju 690-756, South Korea, and School of Chemistry, The University of Manchester, Oxford Road, Manchester, M13 9PL, United Kingdom

Received: March 7, 2008; Revised Manuscript Received: April 15, 2008

This study investigated the decomposition of hydrofluorocarbons (HFCs) having high global warming potentials by using a dielectric-packed-bed nonthermal plasma reactor with barium titanate beads as the packing material. The target HFCs were 1,1,1,2-tetrafluoroethane (HFC-134a) and 1,1-difluoroethene (HFC-132a). The effects of several parameters such as reaction temperature, oxygen content, and initial concentration on the HFC decomposition efficiency were evaluated. There was essentially no temperature dependence of the HFC decomposition efficiency in the range 150−250 °C. The optimum oxygen content for HFC decomposition was found to be about 0.5 vol %. Variations in the initial concentration did not affect the decomposition efficiency. The decomposition products were analyzed, and some decomposition pathways were elucidated. The energy requirements for the decomposition of HFC-134a and HFC-132a were found to be 0.038 and 0.062 mol MJ^{-1}, respectively, based on the initial concentrations of 200 and 120 ppm (parts per million, volumetric).

Introduction

Hydrofluorocarbons (HFCs) being used as replacements for chlorofluorocarbons (CFCs) and hydrochlorofluorocarbons (HCFCs) have high global warming potentials, even though they are not related to ozone depletion. Several technologies are available for the treatment of HFCs, including recovery and reuse, catalytic decomposition, thermal decomposition, and thermal or nonthermal plasma decomposition.[1–5] Among these technologies, nonthermal plasma decomposition can be an effective method when the HFCs exist as impurities, i.e., at low concentration. Fitzsimmons et al.[6] and Ricketts et al.[7] studied the destruction of halogenated carbons such as dichloromethane (CH_2Cl_2) and CFC-12 (CF_2Cl_2) in a dielectric-packed-bed plasma reactor, demonstrating that the fluorocarbons could be efficiently destroyed by the plasma method. The efficiency of the decomposition of the fluorocarbon by the plasma can be enhanced by introducing catalysts or using additives. Futamura and Gurusamy[8] investigated the decomposition of HFC-32 (CH_2F_2) and HFC-23 (CHF_3) using silent discharge plasma or surface discharge plasma in combination with catalysis, and they showed that catalysts such as MnO_2 and TiO_2-SiO_2 could greatly increase the decomposition efficiency. The effects of possible additives including water vapor, oxygen, and hydrogen on the fluorocarbon decomposition was evaluated by Ogata et al.,[5] who found that the enhancement of the decomposition by the additives was due to the fact that they could scavenge the decomposition fragments, preventing the reproduction of stable fluorocarbons. The additives also affected the distribution of the decomposition products. Spiess et al.[9] observed that the addition of oxygen and water vapor largely increased CO_2 production through the breakdown of CFCs.

In addition to the works mentioned above, many studies related to the decomposition of halogenated carbons have been reported so far,[10–16] but only a few studies have addressed chemical aspects such as the identification of reaction products and the decomposition mechanism.[14,15] Moreover, most of the previous studies dealing with the decomposition mechanism were carried out with CFCs and HCFCs, and studies investigating HFCs are scarce in the literature. To determine the optimal reaction conditions and pathways for these processes, the chemical aspects should be thoroughly examined, which can improve the technology for HFC decomposition further. In this study, the decomposition of HFCs using a nonthermal plasma was investigated. The HFCs used were HFC-134a (1,1,1,2-tetrafluoroethane) and HFC-132a (1,1-difluoroethene) whose global warming potentials (GWPs) are 1300 and 350, respectively. The nonthermal plasma reactor of this study was a cylindrical dielectric-packed-bed reactor. The effects of oxygen content, reaction temperature, initial HFC concentration, and energy density (discharge power divided by gas flow rate) on the decomposition were examined, and the results are discussed. Decomposition products from the plasma reactor were identified and quantified by Fourier transform infrared (FTIR) spectroscopy, from which some of the reaction pathways for the decomposition were elucidated.

Experimental Details

The experimental apparatus shown in Figure 1 is basically the same as used in a previous study.[17] The dielectric-packed-bed plasma reactor consisted of a quartz tube of 24-mm inner diameter with two porous electrodes 25 mm apart through which the gas mixture passed. The space between the electrodes was filled with 12 cm^3 of barium titanate dielectric beads (3.5-mm diameter). The plasma reactor was covered with a heating mantle to control the reaction temperature to a desired value. The reaction temperature was varied from 150 to 250 °C. An ac voltage in the range of 16.5−20.5 kV (peak to peak) at a frequency between 10.25−13.25 kHz was applied to the electrodes. The electrical discharge occurred in the barium titanate bed between the two electrodes. The energy density, defined as the ratio of the discharge power to the gas flow rate, was varied up to 160 J L^{-1}.

---

* To whom correspondence should be addressed. E-mail: smokie@cheju.ac.kr (Y.S.M.), j.c.whitehead@manchester.ac.uk (J.C.W.).

[†] Cheju National University.

[‡] The University of Manchester.

10.1021/jp8020084 CCC: $40.75

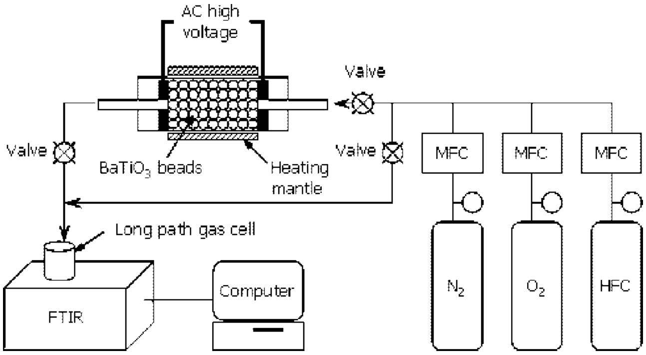

Figure 1. Schematic diagram of the experimental apparatus.

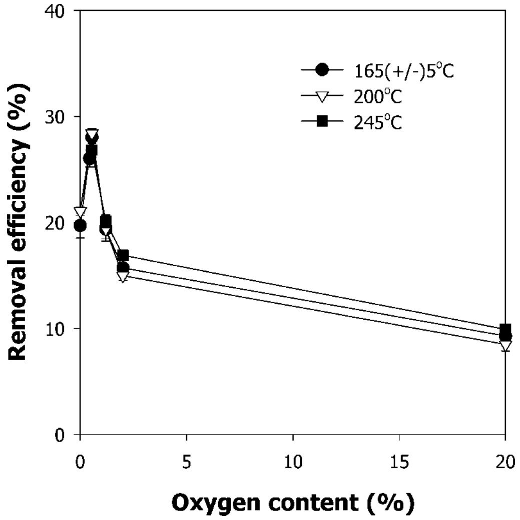

Figure 2. Effects of the oxygen content and the reaction temperature on the HFC-134a decomposition efficiency (feed gas flow rate, 1 L min^{-1}; initial HFC-134a concentration, 200 ppm; energy density, 60 J L^{-1}).

The feed gas was composed of pure nitrogen and pure oxygen and a small amount of hydrofluorocarbon (HFC). All of the gases used were controlled by mass flow controllers (MKS Mass-Flo, MKS Instruments, Andover, MA). The hydrofluorocarbons used as the pollutants were HFC-134a ($C_2H_2F_4$) and HFC-132a ($C_2H_2F_2$). The flow rate of the feed gas was typically 1.0 L min^{-1}. The content of oxygen in the feed gas was changed from 0 to 100 vol %. The initial concentration of HFC-134a was changed in the range of 200−1000 ppm (parts per million, volumetric), and that of HFC-132a was changed in the range of 60−120 ppm. The concentrations of HFC-134a, HFC-132a, and decomposition products were identified and analyzed with an FTIR spectrometer (Shimadzu 8300, Shimadzu Corporation, Kyoto, Japan) equipped with a long-path gas cell (path length = 5 m). The spectra were assigned, and the measured absorbances were converted into concentrations using standard compilations.[18] The HFC decomposition efficiency is defined as $100 \times (C_0 - C)/C_0$, where C_0 and C are the concentrations at the inlet and outlet of the plasma reactor, respectively.

Results and Discussion

HFC-134a Decomposition. Figure 2 shows the effects of the oxygen content of the feed gas and the reaction temperature on the HFC-134a decomposition efficiency. For these experiments, the energy density was fixed at 60 J L^{-1}. As observed, the decomposition efficiency was hardly affected by the reaction temperature in the range 150−250 °C, whereas the effect of the oxygen content was significant. In the absence of oxygen (i.e., in pure nitrogen), the decomposition efficiency was around 20% at all temperatures explored, but it abruptly increased to about 28% when a small amount of oxygen (0.5%) was added to the feed gas. A similar effect was observed for the plasma destruction of dichloromethane, CH_2Cl_2,[6] where the optimum oxygen content for destruction was ~2%. In the absence of oxygen, it is thought that the collisions of HFC-134a with high-energy species such as electrons or excited nitrogen species such as $N_2(A^3\Sigma_u^+)$ and $N(^2D)$ initiate the decomposition

$$C_2H_2F_4 + \text{energetic species} \rightarrow {}^{\bullet}CHF{-}CF_3 + H^{\bullet} \rightarrow CHF{=}CF_2 + HF \quad (1)$$

$$C_2H_2F_4 + \text{energetic species} \rightarrow CH_2F^{\bullet} + CF_3^{\bullet} \quad (2)$$

The electrical discharge produces electrons with an average energy in the range of 5−10 eV, and these electrons can excite nitrogen molecules to higher electronic states. Because the bond strengths for C−H and C−C are 4.3 and 3.6 eV, respectively, reactions 1 and 2 are quite reasonable. Once the HFC-134a molecule is destroyed, the unstable intermediate products can undergo a variety of reactions. The abrupt increase in the decomposition efficiency with a small amount of oxygen is probably because the decomposition products of reactions 1 and 2 can be rapidly scavenged by oxygen species such as $O^{\bullet}$, O_2, and O_3,[19,20] through reactions including

$$CHF{=}CF_2 + O_3 \rightarrow HCOF + COF_2 + O^{\bullet} \quad (3)$$

$$CH_2F^{\bullet} + O_2 \rightarrow CH_2FO_2 \quad (4)$$

$$CF_3^{\bullet} + O_2 \rightarrow CF_3O_2 \quad (5)$$

$$CF_3^{\bullet} + O_3 \rightarrow CF_3O_2 + O^{\bullet} \quad (6)$$

$$CF_3^{\bullet} + O^{\bullet} \rightarrow COF_2 + F^{\bullet} \quad (7)$$

Reactions 3–7, by scavenging the decomposition products, facilitate the primary reactions 1 and 2. In addition, the $F^{\bullet}$ radical formed by reaction 7 is highly reactive in the decomposition of HFC-134a[19]

$$C_2H_2F_4 + F^{\bullet} \rightarrow CF_3{-}CFH^{\bullet} + HF \quad (8)$$

$$CF_3{-}CFH^{\bullet} + O_2 + M \rightarrow CF_3{-}CFHO_2 + M \quad (9)$$

However, contrary to our expectations, further increases in the oxygen content above 0.5% decreased the decomposition efficiency, which indicates that the effects of the oxidative species on the initiation of HFC-134a decomposition are not significant, even though such species can participate in the subsequent reactions. One plausible reason for the lower decomposition efficiency at higher oxygen content might be the high electron affinity of oxygen species, which decrease the concentration of electrons by attaching to them and disturb the energy absorption of nitrogen. Oxygen molecules can also consume the excited nitrogen molecules that can initiate HFC decomposition described in reactions 1 and 2[7]

$$N_2(A^3\Sigma_u^+) + O_2 \rightarrow N_2O + O^{\bullet} \quad (10)$$

In addition, as oxygen is relatively abundant compared to the HFC, the $N^{\bullet}$ radical could react with oxygen rather than with HFC-134a, which decreases the contribution of $N^{\bullet}$ radical to HFC decomposition. Consequently, it can be said that there is an optimum content of oxygen to maximize the decomposition of HFC-134a, which was found to be about 0.5 vol %. At this

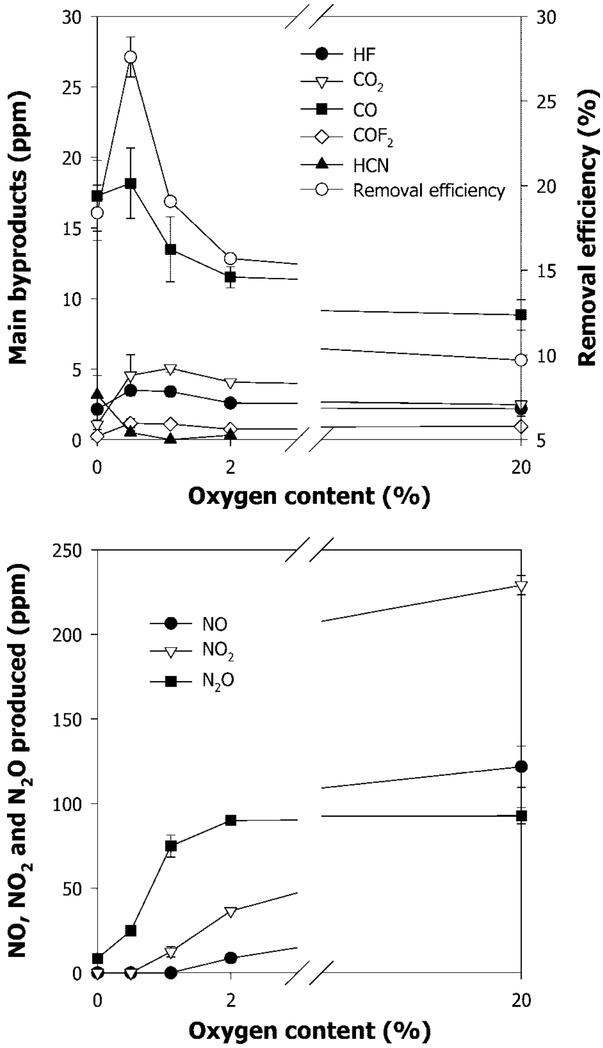

Figure 3. Effects of the oxygen content on the concentrations of byproducts formed from HFC-134a (feed gas flow rate, 1 L min^{-1}, initial HFC-134a concentration, 200 ppm; energy density, 60 J L^{-1}; temperature, 165 °C).

optimum oxygen content, the energy requirement for the decomposition was 0.038 mol MJ^{-1}.

Figure 3 shows the concentrations of byproducts formed from HFC-134a. The most abundant byproducts were nitrogen oxides including nitric oxide (NO), nitrogen dioxide (NO_2), and nitrous oxide (N_2O), which originated from the background gases (i.e., nitrogen and oxygen). The formation of nitrogen oxides by electrical discharge is well known and has been discussed elsewhere.[21,22] In addition to nitrogen oxides, HF, CO, CO_2, COF_2, and HCN were detected by FTIR spectroscopy. Interestingly, even when oxygen was not used, N_2O and CO were detected, suggesting that oxygen can be released from the dielectric beads ($BaTiO_3$). In a previous study, Ogata et al.[5] showed that lattice oxygen atoms can be released from the surface of TiO_2 or Al_2O_3 pellets under plasma discharge, which agrees with our results. Among the identified byproducts in Figure 3, two of the pathways producing HF are reactions 1 and 8. Obviously, the formation of CO and CO_2 results from consecutive reactions of the decomposition products. For instance, the following reactions can form CO and CO_2[20]

$$COF_2 + O(^1D) \rightarrow CO_2 + F_2 \qquad (11)$$

$$COF_2 + F^{\bullet} \rightarrow COF^{\bullet} + F_2 \qquad (12)$$

$$COF^{\bullet} + COF^{\bullet} \rightarrow COF_2 + CO \qquad (13)$$

$$CF_3O_2 + NO \rightarrow CF_3O^{\bullet} + NO_2 \qquad (14)$$

$$CF_3O^{\bullet} + O_2 \rightarrow COF_2 + FO_2 \qquad (15)$$

$$CF_3O^{\bullet} + CO \rightarrow COF_2 + COF^{\bullet} \qquad (16)$$

Here, O(^{1}D) represents the excited oxygen atom. Considering these reactions, carbonyl fluoride (COF_2) is one of the key compounds for the formation of CO and CO_2. Meanwhile, the main reaction pathway for the formation of hydrogen cyanide, HCN, is presumably the reaction of $N^{\bullet}$ radical with 1,1,2-trifluoroethene produced by reaction 1

$$CHF{=}CF_2 + N^{\bullet} \rightarrow HCN + CF_3^{\bullet} \qquad (17)$$

The formation of HCN largely decreases as the oxygen content increases, as the $N^{\bullet}$ radical reacts preferentially with abundant compounds such as O_2, NO, NO_2, and so on.

$$N^{\bullet} + O_2 \rightarrow NO + O^{\bullet} \qquad (18)$$

$$N^{\bullet} + NO_2 \rightarrow N_2O + O^{\bullet} \qquad (19)$$

$$N^{\bullet} + NO \rightarrow N_2 + O^{\bullet} \qquad (20)$$

Among these reactions, reaction 18 is believed to mainly consume $N^{\bullet}$ radicals because the concentration of oxygen is much higher than those of other compounds. Again, this behavior parallels that observed for the decomposition of dichloromethane where HCN was observed as a product only in the absence of oxygen.[6]

The effects of the reaction temperature on the formation of NO and NO_2 in the presence and of HFC-134a are presented in Figure 4. In these experiments, the oxygen content was adjusted to 20 vol %, and the energy density was fixed at 60 J L^{-1}. Without HFC-134a, the main reactions related to the oxidation of NO to NO_2 are[21,22]

$$O^{\bullet} + O_2 + M \rightarrow O_3 + M \qquad (21)$$

$$NO + O_3 \rightarrow NO_2 + O_2 \qquad (22)$$

$$NO + O^{\bullet} \rightarrow NO_2 \qquad (23)$$

Reactions 21 and 23 have an inverse temperature dependence. Furthermore, the rate of ozone decomposition into oxygen atom and molecular oxygen largely increases with the temperature. This is why the ratio of NO_2 to NO decreased as the reaction temperature increased. The presence of HFC-134a can affect the oxidation of NO to NO_2, as is the case for most hydrocarbons.[23] At the same temperature, the ratio of NO_2 to NO was higher in the presence of HFC-134a than in its absence, as has been previously seen for other halocarbons.[24] This result implies that intermediate products formed by reactions 3–9 are involved in the oxidation of NO, as in reaction 14. In addition to reaction 14, other possible reactions include

$$CH_2FO_2 + NO \rightarrow CH_2FO^{\bullet} + NO_2 \qquad (24)$$

$$CF_3{-}CFHO_2 + NO \rightarrow CF_3{-}CFHO^{\bullet} + NO_2 \qquad (25)$$

$CH_2FO^{\bullet}$ and $CF_3{-}CFHO^{\bullet}$ produced by reactions 24 and 25 can be further degraded by oxygen to form various products as in the following reactions[19,20,25]

$$CF_3{-}CFHO + O_2 \rightarrow CF_3{-}COF^{\bullet} + HO_2 \qquad (26)$$

$$CF_3{-}CFHO \rightarrow CF_3^{\bullet} + HCOF \qquad (27)$$

$$CF_3{-}COF^{\bullet} \rightarrow COF + CF_3^{\bullet} \quad (28)$$

$$CF_3{-}COF^{\bullet} \rightarrow COF_2 + CF_2^{\bullet} \quad (29)$$

$$CF_3{-}COF^{\bullet} \rightarrow CO + CF_4 \quad (30)$$

$$CF_2^{\bullet} + CF_2^{\bullet} \rightarrow C_2F_4 \quad (31)$$

$$CF_3^{\bullet} + CF_3^{\bullet} \rightarrow C_2F_6 \quad (32)$$

$$COF^{\bullet} \rightarrow CO + F^{\bullet} \quad (33)$$

Reactions 3 and 27 suggest that, in addition to COF_2, formyl fluoride (HCOF) can be formed, but in this study, HCOF could not be quantified because CO_2, HCOF, and HFC-134a overlapped at 666−668 cm^{-1} in the FTIR spectra.

Figure 5 shows the carbon balance between the HFC-134a molecules removed (open circles) and the carbon-containing products identified (solid circles). As discussed above, many reactions producing a variety of products are involved in the decomposition of HFC-134a, and thus, it is not possible to obtain a good carbon balance. As can be seen, the concentration of carbon identified tended to decrease as the oxygen content increased, but the relative amount of carbon identified (i.e., the ratio of the black circle symbols to the white circle symbols) was higher at higher oxygen content because oxidative species such as O, O_2, and O_3 necessarily convert intermediate products into CO, CO_2, and COF_2.

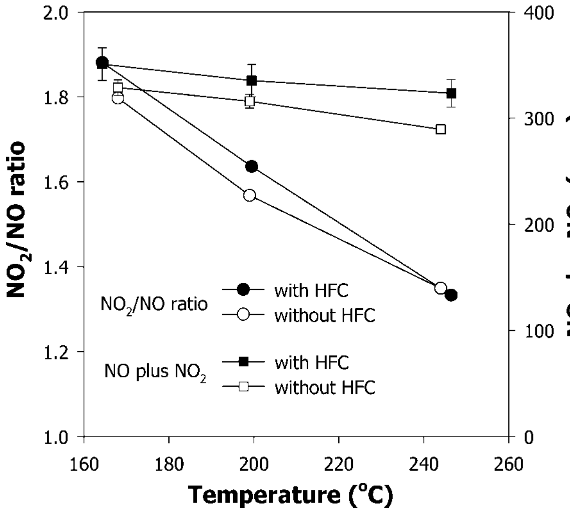

Figure 4. Effects of the reaction temperature on the formation of NO and NO_2 in the presence and in the absence of HFC-134a (feed gas flow rate, 1 L/min; initial HFC-134a concentration, 200 ppm; energy density, 60 J L^{-1}; oxygen content, 20 vol %).

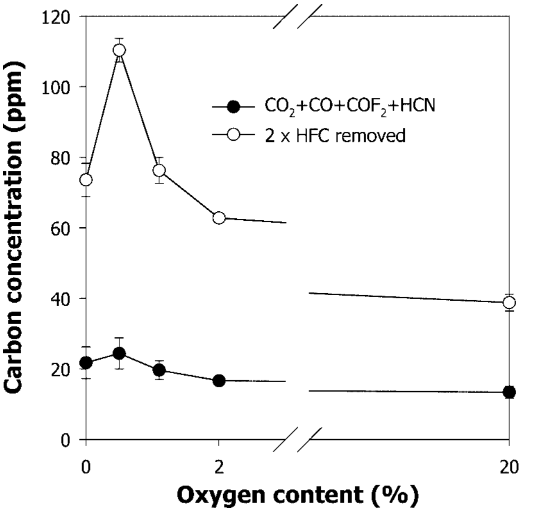

Figure 5. Carbon balance between the HFC-134a molecules removed (open circles) and the carbon-containing products identified (solid circles) (feed gas flow rate, 1 L min^{-1}; initial HFC-134a concentration, 200 ppm; energy density, 60 J L^{-1}; temperature, 165 °C).

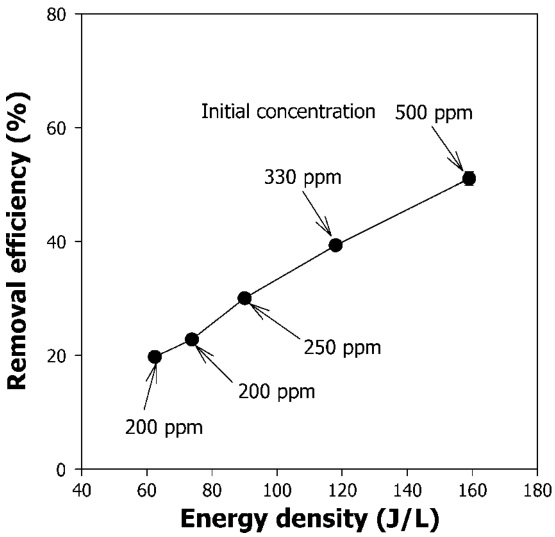

Figure 6. Dependence of the HFC-134a decomposition efficiency on the energy density and initial concentration in the presence of nitrogen as the background gas (temperature, 165 °C).

The effect of the initial HFC-134a concentration on the decomposition efficiency was examined with either N_2 or O_2 as the background gas. In the range of 200−1000 ppm, the decomposition efficiency did not depend on the initial concentration. At an energy density of 60 J L^{-1}, the decomposition efficiency was about 20% with N_2 and about 9% with O_2, regardless of the initial concentration. For further investigation of this unusual phenomenon, both the energy density and the initial HFC-134a concentration were varied with nitrogen as the background gas. Figure 6 summarizes the results for changes in the energy density and initial concentration. As observed, the decomposition efficiency linearly increased with the energy density, despite the fact that the initial concentration also increased. These results provide valuable information for understanding the mechanism of HFC-134a decomposition. If radical reactions played an important role in the decomposition, the efficiency of decomposition would depend on the initial concentration because a limited amount of radicals would be formed at a particular energy density. According to the calculations using a Boltzmann equation solver BOLSIG code (Siglo), it was found that most of the energy delivered to the gas was consumed in excitation of the gas molecules rather than radical production. Thus, it is reasonable to infer that the excited nitrogen molecules play a more important role in HFC-134a decomposition than the radical species do. Therefore, when the amount of excited nitrogen molecules is abundant, the effects of the initial concentration can vanish.

Figure 7 depicts some of the reaction pathways involved in HFC-34a decomposition in the presence of nitrogen and oxygen. The reaction pathways were assumed from the identified byproducts enclosed in boxes and include suggestions. The elimination of hydrogen fluoride and the reaction with $F^{\bullet}$ radical can initiate HFC-134a decomposition. As described above, oxidative species such as $O^{\bullet}$, O_2, and O_3 scavenge the decomposition products to eventually form carbon oxides. However, at high oxygen concentrations beyond a certain value,

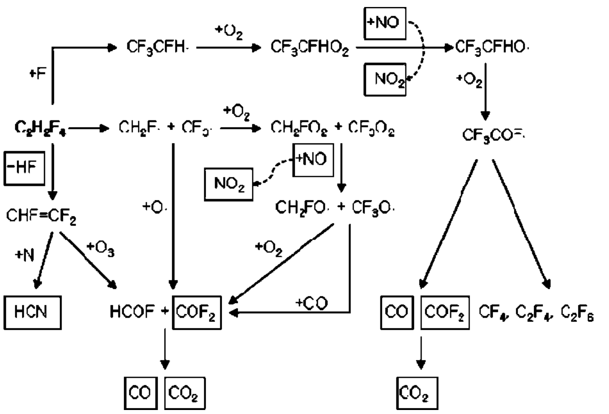

Figure 7. HFC-134a decomposition mechanisms deduced from the identified byproducts.

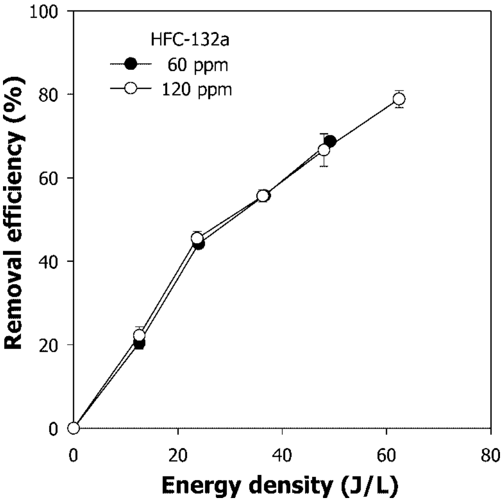

Figure 8. Effects of the energy density on HFC-132a decomposition at different initial concentrations (feed gas flow rate, 1 L min^{-1}; oxygen content, 20 vol %; temperature, 165 °C).

excited nitrogen species such as $N_2(A^3\Sigma_u^+)$ and $N(^2D)$ that are used to initiate the decomposition are consumed by reaction with oxygen, which results in the observed decrease in the decomposition efficiency.

HFC-132a Decomposition. Figure 8 presents the results for the decomposition of HFC-132a ($C_2H_2F_2$) that were obtained by varying the energy density at different initial concentrations. The energy density was varied by changing the discharge power from 0.2 to 1.0 W at a constant feed-gas flow rate of 1.0 L min^{-1}. As in the case of HFC-134a, the efficiency of HFC-132a decomposition was not dependent on the initial concentration, but it was dependent only on the energy density. This result implies that the amount of the reactive species produced in the plasma reactor capable of initiating the decomposition is much greater than that for HFC-132a. The formation of nitrogen oxides results from the background gases O_2 and N_2, and their pathways are discussed above. The main carbon-containing byproducts identified were CO, CO_2, and COF_2 (see Figure 9). Some plausible reactions for the formation of these oxidized compounds are as follows[20]

$$CH_2{=}CF_2 + O_3 \rightarrow CH_2O + COF_2 + O^\bullet \tag{34}$$

$$CH_2{=}CF_2 + O^\bullet \rightarrow COF_2 + CH_2^\bullet \tag{35}$$

$$CH_2^\bullet + O_2 \rightarrow CO + H_2O \tag{36}$$

$$COF_2 + O(^1D) \rightarrow CO_2 + F_2 \tag{11}$$

$$CH_2O + O \rightarrow OH^\bullet + H^\bullet + CO \tag{37}$$

$$CH_2O + NO \rightarrow HNO + HCO \tag{38}$$

$$HCO + O_2 \rightarrow CO_2 + OH^\bullet \tag{39}$$

$$HCO + O_2 \rightarrow CO + HO_2\bullet \tag{40}$$

$$HCO + O^\bullet \rightarrow CO + OH^\bullet \tag{41}$$

$$HCO + O^\bullet \rightarrow CO_2 + H^\bullet \tag{42}$$

As mentioned above, most of the energy delivered to the gas is used to excite the gas molecules, and thus HFC-132a can also be decomposed as a result of collision with an excited nitrogen molecule

$$C_2H_2F_2 + N_2(A^3\Sigma_u^+) \rightarrow H^\bullet + CHCF_2 \rightarrow HF + C_2HF \tag{43}$$

According to a comparison of Figure 6 with Figure 8, the decomposition of HFC-132a requires less energy than that of HFC-134a. According to previous studies, alkenes having double bonds such as ethene and propene are more easily decomposed by electrical discharge than alkanes such as ethane and propane.[26,27] The results in Figures 6 and 8 can be explained from the same point of view. Moreover, in the case of $CH_2{=}CF_2$, two electronegative fluorine atoms are attached to the same carbon atom, thus weakening the C=C double bond. This can also partly explain why the decomposition of HFC-132a consumes much less energy than that of HFC-134a. Judging from the decomposition efficiency of 80% at the initial concentration of 120 ppm, the energy requirement for HFC-132a decomposition was calculated to be 0.062 mol MJ^{-1}. Note that the energy requirement will be higher at higher initial concentration because the decomposition efficiency does not depend on initial concentration.

Some of the reaction pathways involved in the decomposition of HFC-132a are depicted in Figure 10; they were deduced from the identified decomposition products enclosed in boxes. The reaction pathways include suggestions because all decomposition products were not identified. HFC-132a decomposition can be initiated by various reactive species including excited nitrogen molecules, ozone, oxygen atoms, and nitrogen atoms. Excited nitrogen molecules can eliminate hydrogen fluoride from HFC-

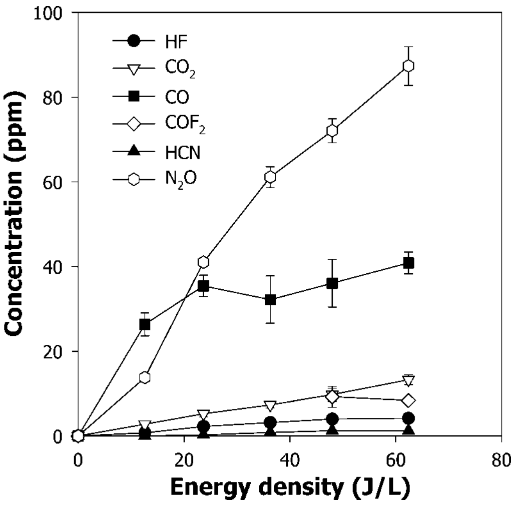

Figure 9. Byproduct distribution as a function of energy density (feed gas flow rate, 1 L min^{-1}; oxygen content, 20 vol %; initial HFC-132a concentration, 120 ppm; temperature, 165 °C).

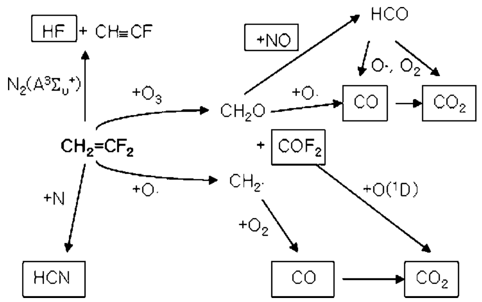

Figure 10. HFC-132a decomposition mechanisms deduced from the identified byproducts.

132a. Ozone readily adds to the double bond, yielding formaldehyde and carbonyl fluoride, which are typical products in reactions of alkenes with ozone. Oxygen atoms can also lead to the breaking of the double bond, as in reaction 35. The decomposition products formed by these reactions are further oxidized by oxidative species such as O, O_2, and O_3 to produce CO and CO_2.

Conclusions

A dielectric-packed-bed plasma reactor with barium titanate beads was employed to destroy the hydrofluorocarbons HFC-134a and HFC-132a. The parametric study showed that the decomposition efficiency did not depend on the reaction temperature or the initial HFC concentration. On the other hand, the oxygen content was found to have a significant influence on the decomposition efficiency, and the optimum oxygen content is about 0.5 vol %. The results obtained from the parametric study and the decomposition products identified reveal that HFC-134a decomposition is initiated by energetic species such as excited molecules and atoms, which is followed by rapid scavenging of the intermediate products by oxidative species. In the case of HFC-132a, ozone and oxygen atoms can also initiate the decomposition, because these species readily add to the double bond, causing it to break. The energy requirements for the decomposition of HFC-134a and HFC-132a were 0.038 and 0.062 mol MJ^{-1}, respectively. Although the decomposition products identified in this study suggest some reaction pathways for HFC decomposition, further work is needed to refine the decomposition mechanism. In addition, use of the nonthermal plasma in combination with catalysis or another technology might be worth consideration for improving the decomposition efficiency.

Acknowledgment. Support of this work by the U.K. Engineering and Physical Sciences Research Council and the award of an EC Marie Curie IIF to V.D. is gratefully acknowledged.

References and Notes

(1) Takita, Y.; Tanabe, T.; Ito, M.; Ogura, M.; Muraya, T.; Yasuda, S.; Nishiguchi, H.; Shihara, T. *Ind. Eng. Chem. Res.* **2002**, *41*, 2585.

(2) Takizawa, K.; Takahashi, A.; Tokuhashi, K.; Kondo, S.; Sekiya, A. *J. Fluorine Chem.* **2006**, *127*, 1547.

(3) Ohno, M.; Ozawa, Y.; Mizuno, A.; Ono, T. *Res. Inst. Environ. Technol.* **2007**, *36*, 427.

(4) Ohno, M.; Ozawa, Y.; Ono, T. *Int. J. Plasma Environ. Sci. Technol.* **2007**, *1*, 159.

(5) Ogata, A.; Kim, H.-H.; Futamura, S.; Kushiyama, S.; Mizuno, K. *Appl.Catal. B: Environ.* **2004**, *53*, 175.

(6) Fitzsimmons, C.; Ismail, F.; Whitehead, J. C.; Wilman, J. J. *J. Phys. Chem. A* **2000**, *104*, 6032.

(7) Ricketts, C. L.; Wallis, A. E.; Whitehead, J. C.; Zhang, K. *J. Phys. Chem. A* **2004**, *108*, 8341.

(8) Futamura, S.; Gurusamy, A. *J. Electrostatics* **2005**, *63*, 949.

(9) Spiess, F.-J.; Chen, X.; Brock, S. L.; Suib, S. L.; Hayashi, Y.; Matsumoto, H. *J. Phys. Chem. A* **2000**, *104*, 11111.

(10) Chang, M. B.; Yu, S. J. *Environ. Sci. Technol.* **2001**, *35*, 1587.

(11) Kang, H.-C. *J. Ind. Eng. Chem.* **2002**, *8*, 488.

(12) Futamura, S.; Einaga, H.; Zhang, A. *IEEE Trans. Ind. Appl.* **2001**, *37*, 978.

(13) Yen, S. J.; Chang, M. B. *Plasma Chem. Plasma Process.* **2001**, *21*, 469.

(14) Wallis, A. E.; Whitehead, J. C.; Zhang, K. *Appl. Catal. B* **2007**, *74*, 111.

(15) Arkady, G.; Ogata, A.; Futamura, S.; Mizuno, K. *J. Phys. Chem. A* **2003**, *107*, 8859.

(16) Park, J.-Y.; Park, J.-G.; Kim, J.-S.; Rim, G.-H.; Kim, K.-S. *IEEE Trans. Plasma Sci.* **2003**, *31*, 1349.

(17) Demidyuk, V.; Whitehead, J. C. *Plasma Chem Plasma Process.* **2007**, *27*, 85.

(18) Hanst, P. L.; Hanst, S. T. *Infrared Spectra for Quantitative Analysis of Gases*; Infrared Analysis Inc.: Anaheim, CA, 1993.

(19) Møgelberg, T. E.; Sehested, J.; Wallington, T. J.; Nielsen, O. J. *Int. J. Chem. Kinet.* **1997**, *29*, 209.

(20) NIST Chemical Kinetics Database, version 2Q98; National Institute of Standards and Technology (NIST): Gaithersburg, MD, 1998.

(21) Mok, Y. S.; Kim, J. H.; Ham, S. W.; Nam, I. *Ind. Eng. Chem. Res.* **2000**, *39*, 3938.

(22) Tas, M. A.; van Hardeveld, R.; van Veldhuizen, E. M. *Plasma Chem. Plasma Process.* **1997**, *17*, 371.

(23) Sathiamoorthy, G.; Kalyana, S.; Finney, W. C.; Clark, R. J.; Locke, B. R. *Ind. Eng. Chem. Res* **1999**, *38*, 1844.

(24) Harling, A. M.; Whitehead, J. C.; Zhang, K. *J. Phys. Chem. A* **2005**, *109*, 11255.

(25) Labelle, C. B.; Karecki, S. M.; Reif, R.; Gleason, K. K. *J. Vac. Sci. Technol. A* **1999**, *17*, 3419.

(26) Mok, Y. S.; Nam, C. M.; Cho, M. H.; Nam, I.-S. *IEEE Trans. Plasma Sci.* **2002**, *30*, 408.

(27) Yamamoto, T. *J. Hazard. Mater.* **1999**, *67*, 165.

JP8020084